Kinetics of sonophotocatalytic degradation of an anionic dye nigrosine with doped and undoped zinc oxide

Srishti Kumawat, Kiran Meghwal, Sudhish Kumar, Rakshit Ameta and Chetna Ameta

ABSTRACT

The current research focuses on the photocatalytic, sonocatalytic and sonophotocatalytic degradation of nigrosine dye with nitrogen-doped and undoped zinc oxide powders.

The sonophotocatalytic degradation of dye was found to occur at a higher rate than during photo- or sonocatalytic processes. Nitrogen-doped and undoped zinc oxide powders were synthesized by a wet chemical method. Further, scanning electron microscopy (FESEM), electron dispersive X-ray (EDX), X-ray diffraction (XRD), Fourier-transform infrared spectroscopy (FTIR), UV-VIS spectroscopy (UV-VIS) and transmission electron microscopy (TEM) were used for the characterization of N-doped ZnO. The kinetics of nigrosine degradation were also studied and the results indicated that the degradation kinetics of nigrosine followed the first-order kinetics. The rate constant and the percentage of degradation were found to be highest, 7.33×10^{-4} (s^{-1}) and 92% respectively, for sonophotocatalytic process after 90 min of reaction. Due to an increase in the available surface area or active sites of the catalyst, a higher rate constant and degradation efficiency was observed in the sonophotocatalytic system than in the photocatalysis system.

Key words | nigrosine dye, nitrogen-doped ZnO, photocatalysis, sonocatalysis, sonophotocatalysis

Srishti Kumawat
Kiran Meghwal
Chetna Ameta (corresponding author)
Photochemistry Laboratory, Department of Chemistry,
University College of Science, M. L. Sukhadia University,
Udaipur 313002, Rajasthan,
India
E-mail: *chetna.ameta@yahoo.com*

Sudhish Kumar
Department of Physics,
University College of Science, M. L. Sukhadia University,
Udaipur 313002, Rajasthan,
India

Rakshit Ameta
Department of Chemistry,
J. R. N. Rajasthan Vidyapeeth (Deemed-to-be University),
Udaipur 313001, Rajasthan,
India

INTRODUCTION

A number of treatment methods, both physical and chemical, have been reported for treatment of dye effluents (Robinson *et al.* 2001; Saratale *et al.* 2011). Of them, an effective and widely used chemical treatment method is advanced oxidation processes (AOPs), which finds application in removal of recalcitrant organic components from textile, municipal and industrial wastewater without releasing any secondary waste in the environment (Azbar *et al.* 2004; Comninellis *et al.* 2008). Moreover, it has received great attention due to increasing eco-conservation concerns. Amongst other AOPs, sonocatalytic degradation is considered as a rather new technology for wastewater treatment. In this process, the ultrasound irradiation of the reaction system drives the transient collapse of cavitation bubbles, which further produces the $^{\bullet}OH$ radicals (Shah *et al.* 1990; Chakma & Moholkar 2013). However, the resulting radicals from sonocatalysis alone cannot achieve the desired level of degradation of the pollutants (Zhu *et al.* 2013; Khataee *et al.* 2015). In order to overcome this limitation, research is in progress in many laboratories to combine sonocatalysis with other AOP techniques (Chen & Smirniotis 2002; Gogate 2008; Joseph *et al.* 2009; Torres-Palma *et al.* 2010; Anju *et al.* 2012). Sonophotocatalysis enhances the degradation rate by combining ultrasound waves and a semiconductor photocatalyst and this has led to it being the preferred method for degrading organic pollutants among all other oxidation processes. Here, the organic compounds undergo photocatalytic degradation through the formation of $^{\bullet}OH$ radicals on the photocatalyst. During the photochemical reactions, cavitation bubbles are formed which increase the pyrolysis of H_2O molecules and formation of $^{\bullet}OH$ radicals. The generation of $^{\bullet}OH$ radicals gets enhanced in sonophotocatalysis, primarily due to the synergistic effect between sonolysis (US) and photocatalysis (UV). This further leads to an increase in the rate of degradation of organic pollutants.

Recently, the application of heterogeneous photocatalysis in drinking water treatment, environmental clean-up and health and industrial applications has been on the rise. It uses the semiconductor materials as photocatalysts for

doi: 10.2166/wst.2019.396

the removal of ambient concentrations of organic and inorganic species from aqueous or gas phase systems (Al-Ekabi & Serpone 1988; Xu *et al.* 2009). TiO_2 has been the most effective photocatalyst for a wide range of organic chemical degradation. However, there have been cases where ZnO has been more effective than TiO_2, which has recently led to its acceptance as an effective photocatalyst. The fact that ZnO is a representative of the metal oxide class has also led to incremental studies in the field of electrochemistry and catalysis. The ZnO nanoparticle has received great attention for its use in eliminating environmental pollution due to reasons such as low cost of production, responsiveness to UV light having a band gap range of 3.2–3.3 eV and high photoactivity in several photochemical and photoelectron-chemical processes (Hoffman *et al.* 1995; Kandavelu *et al.* 2004; Periyat & Ullattil 2015; Seo & Shin 2015). The ZnO nanostructure finds use in catalytic reaction process because of its large surface area and high catalytic activity. Doping ZnO with anionic or non-metal dopants like C, N, F, S, and P makes it active in visible light region (Mollavali *et al.* 2018; Singh *et al.* 2018; Su *et al.* 2018). The anionic or non-metal-doped catalysts are much better than cationic or metal-doped catalysts because their impurity states are quite close to the valence band (VB) edge and their role is minimum as recombination centres. Nowadays, for the nanostructure level production of oxides, sulphides etc., microwave assisted methods are being widely used. It is mainly due to the capabilities exhibited by these methods, which are fast reaction, low cost, environmentally friendly, morphology sustainability of particles and short time to attain suitable temperature. Therefore, microwave assisted methods can be considered superior to most of the other reported methodology. (Kooti & Sedeh 2013; Pimentel *et al.* 2014). Nigrosine dye (NG), which is a mixture of artificial black dyes (CI 50420, acid black 2) is prepared by heating an aniline, nitrobenzene and aniline hydrochloride mixture in the presence of a catalyst like copper or iron. It is a water-soluble anionic dye and finds industrial applications in marker-pen inks and colorant for varnishes (Willey *et al.* 2009). In biology field, its main applications are in negative staining bacteria as well as the capsule-containing fungus.

In this paper, the comparative investigation of sonocatalysis, photocatalysis and sonophotocatalysis has been addressed with a dual approach: (1) microwave–assisted synthesis and characterization of N-doped ZnO nanoparticles (NZO); and (2) discernment of physical mechanism of sonocatalysis, photocatalysis and sonophotocatalysis with N-doped ZnO nanoparticles. For model reaction system, decolorization process of textile dyes, viz. anionic dye nigrosine has been used.

EXPERIMENTAL

This section is separated into three parts.

Materials and methods

Zinc acetate dihydrate (ZAD) (SRL), hydrazine dihydrochloride (Thomas Baker), and NH_4OH solution were used in the present investigation. Nigrosine (NG) (HiMedia Laboratories Limited, Mumbai, India) was chosen as a representative model compound. All the chemicals used were of laboratory grade. All solutions were prepared in distilled water.

Preparation of N-doped zinc oxide

Synthesis of NZO (N-doped ZnO) nanoparticles was carried out by the wet chemical method using a microwave synthesizer. Zinc acetate dihydrate ($Zn(CH_3{\cdot}COO)_2.2H_2O$) was doped with hydrazine dihydrochloride ($N_2H_4.2HCl$) which was taken as a source of N. 0.5 M zinc acetate dihydrate (ZAD) and 0.1 M hydrazine dihydrochloride were mixed in deionized water and magnetically stirred until completely dissolved.

The required amount of ammonia solution was then added drop by drop to the prepared solution with constant stirring until a clear solution was obtained. The prepared solution was irradiated with a microwave synthesizer (Electrolux-EM 20 EC) for 3–4 min at 900 watts (525 °C). After 3 minutes, the precipitate settled down at the bottom of the container and was allowed to cool down overnight in alcohol. The precipitate was collected with the help of Whatman filter paper in a Buchner funnel and was repeatedly washed with distilled water and alcohol. It was then dried in an oven for 2–3 hours at 110 °C.

Preparation of zinc oxide

For undoped ZnO (ZO), the above synthesis procedure was followed as it is, with the exception of hydrazine dihydrochloride.

The crystallinity of NZO powder was determined by X-ray diffraction (XRD) using Rigaku Ultima IV with Cu Kα radiation in the range $2\theta = 10$–$90°$. The accelerating voltage was 40 kV and the applied current was at 40 mA rating. Data obtained from XRD measurements were matched with standard JCPDS data (card no. 00-005-0664) and indexing of all well-defined diffraction peaks was done

accordingly. The morphology of the synthesized nanoparticles of NZO was studied by field emission scanning electron microscopy (FESEM). It was recorded on the Hitachi SU8010 FESEM. The transmission electron microscopy (TEM) study of the microstructure of NZO was carried out on a TEM-Tecnai G2 20 instrument. The examination of nanoparticles was done by recording their IR spectra using a Bruker OPUS 7.5.18 Fourier-transform infrared (FTIR) spectrophotometer. The wavelength of the UV–visible reflectance mode spectra of prepared nanoparticles was recorded in the wavelength range of 200–800 nm, using a Perkin-Elmer Lambda-750 UV–visible spectrophotometer.

Photocatalytic, sonocatalytic and sonophotocatalytic activity

In this study, degradation of NG dye (used as a pollutant) was investigated in the presence of NZO nanoparticles using 200 W tungsten lamp (photocatalysis) and ultrasonic bath (sonocatalysis) systems separately and simultaneously (sonophotocatalysis). A stock solution of NG (1.0×10^{-3} mol L^{-1}) was prepared in double distilled water. The reaction suspension was prepared by adding 0.20 g of the photocatalyst in 50 mL of 3.0×10^{-5} mol L^{-1} NG solution. To establish an adsorption–desorption equilibrium on the photocatalyst before light irradiation, the mixed solution was kept in a dark environment for an hour. For the measurement of light intensity (in the unit of mW cm^{-2}), a solarimeter (Surya Mapi Model CEL 201) was used. To measure the maximum light intensity, the distance between the exposed surface of the reaction vessel and the filament of the lamp was varied. The maximum rate of degradation of NG dye was found at 60.0 mW cm^{-2} for both doped and undoped ZnO. The sonocatalytic and sonophotocatalytic degradation was estimated by catalyst with a rectangular shaped ultrasonic bath (Systronics Model 392) filled with water and operated at a fixed frequency of 40 kHz and an ultrasonic power of 200 W. All runs were performed under atmospheric conditions and by continuously stirring the reaction mixture. A water filter was deployed to cut off the thermal radiations. The pH of the reaction mixture was measured through a digital pH meter (Systronics Model 335). 0.1 N sulfuric acid and 0.1 N sodium hydroxide solutions, which were previously standardized, were added to adjust the pH of the solution. Prior to measurement of optical density, NZO particles were separated using a centrifuge. A UV-VL spectrophotometer 2,371 was used at different time intervals to measure the optical density of reaction mixture at 570 nm (λ_{max} of nigrosine).

Quality parameters of water

Different quality parameters like dissolved oxygen (DO), salinity, TDS, conductivity and pH of polluted and treated water were determined by using a water analyser (Systronics Model 371). Chemical oxygen demand (COD) of NG dye solution was estimated before and after the sonophotocatalytic treatment with a standard dichromate method using COD digester. The following expression was used to calculate the percentage of photodegradation efficiency (η):

$$\eta = [(COD_{Initial} - COD_{Final})/COD_{Initial}] \times 100 \quad (1)$$

RESULTS AND DISCUSSION

Characterization of sample

Figure 1 presents the XRD pattern of N-doped ZnO. Bragg reflections at 31.7°, 34.3°, 36.2°, 47.4°,56.5°, 62.7° and 68.0° are indexed as (100), (002), (101), (102), (110), (103) and (112) in the wurtzite-type hexagonal symmetry. Further Rietveld refinement of the XRD pattern was carried out in the space group $P6_3$ MC (No. 186). Figure 1 illustrates excellent fitting of the XRD profiles. Presence of all the fundamental Bragg reflection in the XRD pattern, absence of reflections from any impurity phase, sharp and intense peaks showed that N-doped ZnO formed in single phase wurtzite type hexagonal symmetry without any impurity within the detection limit. The obtained values of the hexagonal lattice parameters are formed to be a = 3.2555 and c = 5.2158. These values are very close to those reported

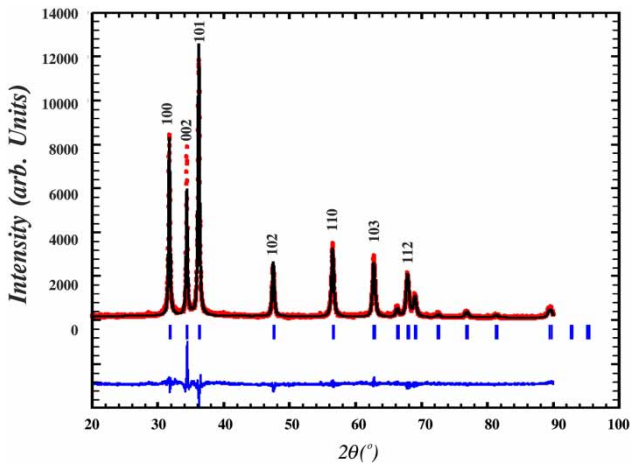

Figure 1 | XRD pattern of N-doped ZnO.

for pure ZnO. Thus N doping in ZnO does not disturb the crystal structures.

Significant broadening in the Bragg reflection is spin, which is signature of nanocrystalline nature of the prepared sample. The average crystallite size was estimated using 'Scherrer's' formula. The estimated crystallite size of N-doped ZnO and pure ZnO was found to be ~32 nm and ~35 nm respectively.

The FESEM micrographs of these synthesized samples are shown in Figure 2. Figure 2(a) shows NZO particles are uniform and have good regularity overall on surface observation. The nanorods formed are either separate or mostly occur as a cluster of agglomerated rods (Figure 2(b) and 2(c)). These rods assemble to form flower-like structures and these nanorods have a 'pencil-like tip' at both ends (Figure 2(d)). Upon closer examination, we observe that the nanorods are hexagonal in shape (as shown in Figure 2(e)).

Electron dispersive X-ray (EDX) spectroscopy was performed to confirm N presence and compositional analysis of nanoparticles. The obtained result of NZO was found to be 0.80 w% for N, 19.64 w% for O, 85.86 w% for zinc. This result confirms the content of the N incorporated in ZnO.

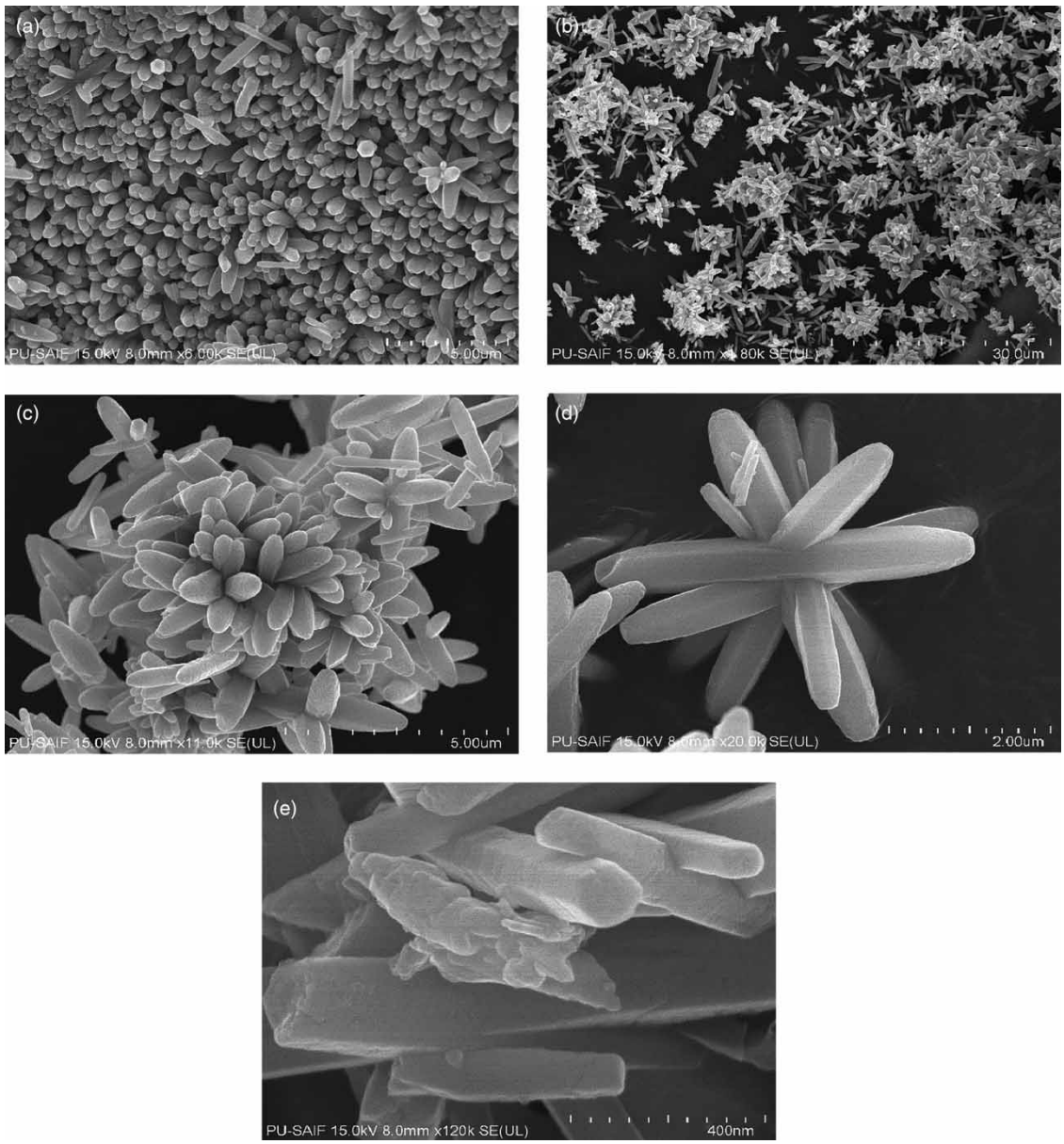

Figure 2 | FESEM of N-doped ZnO at a distance of (a) 5.00 μm, (b) 30.0 μm, (c) 5.00 μm, (d) 2.00 μm, (e) 400 nm.

The TEM image of the N-doped ZnO powder is shown in Figure 3. Selected-area electron diffraction (SAED) pattern in Figure 3(a) and 3(b) and TEM image (Figure 3(c)) reveal that the nanorods are single crystalline and no amorphous products are found on the surface of the nanorods. As per the estimate from the TEM image, the size of the primary particles was about 20–50 nm which is in good agreement with the value (31.99 nm), calculated from XRD pattern using the Scherrer equation.

FTIR spectra of NZO showed an intense, broad peak near 3,360 cm^{-1} which represents the O-H stretching vibration (Seguel *et al.* 2005). Two peaks at 1,390 and 1,502 cm^{-1} for NZO sample may correspond to the vibration of the Zn-N bonds, representing the successful doping of ZnO with nitrogen (Lu *et al.* 2006). This spectra also shows absorption peaks below 600 cm^{-1}, which correspond to the characteristic absorption of Zn-O bond in zinc oxide as shown in

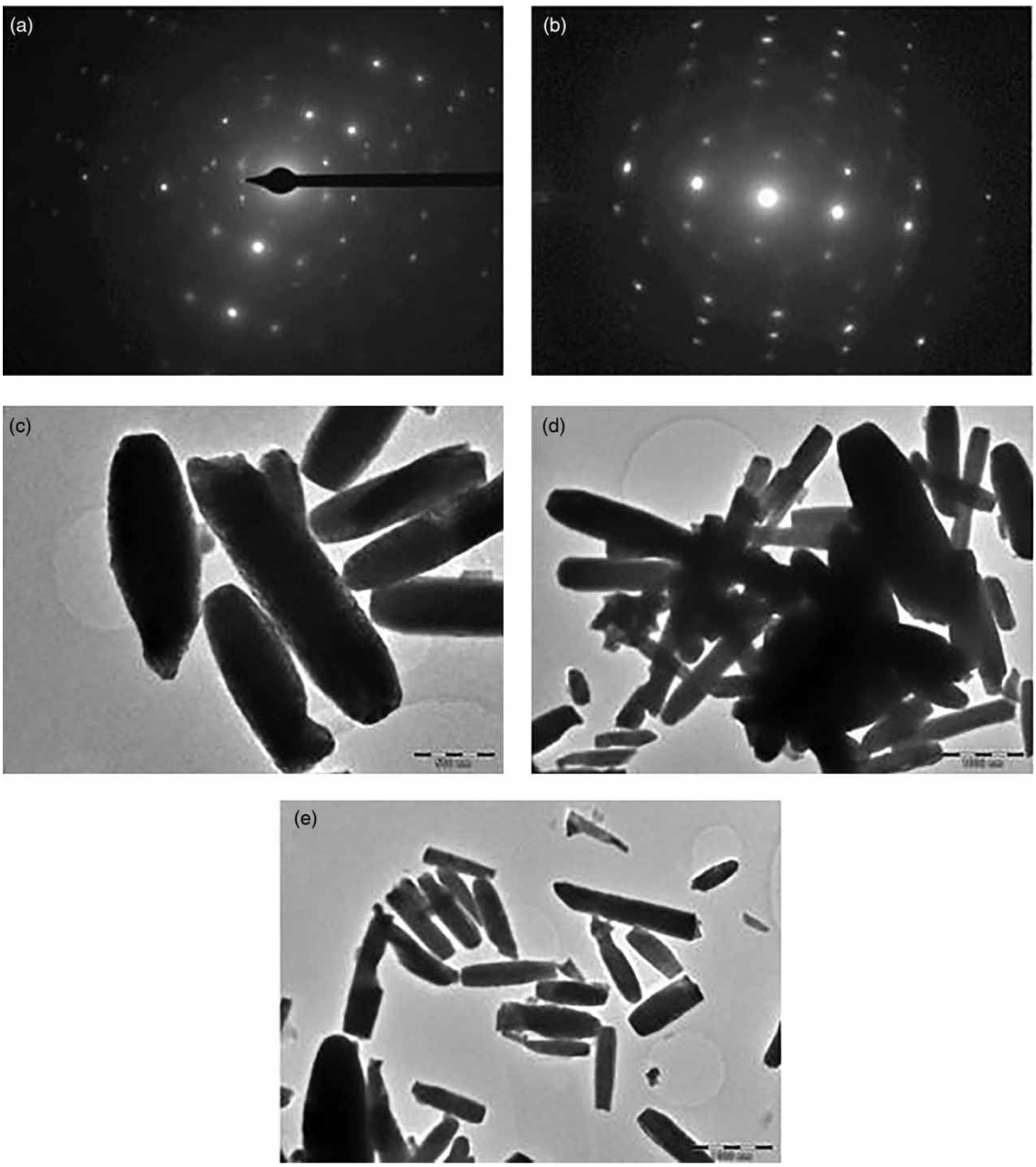

Figure 3 | TEM images of N-doped ZnO where (a) and (b) show SAED pattern; (c) captured at 500 nm and (d) and (e) captured at 1,000 nm.

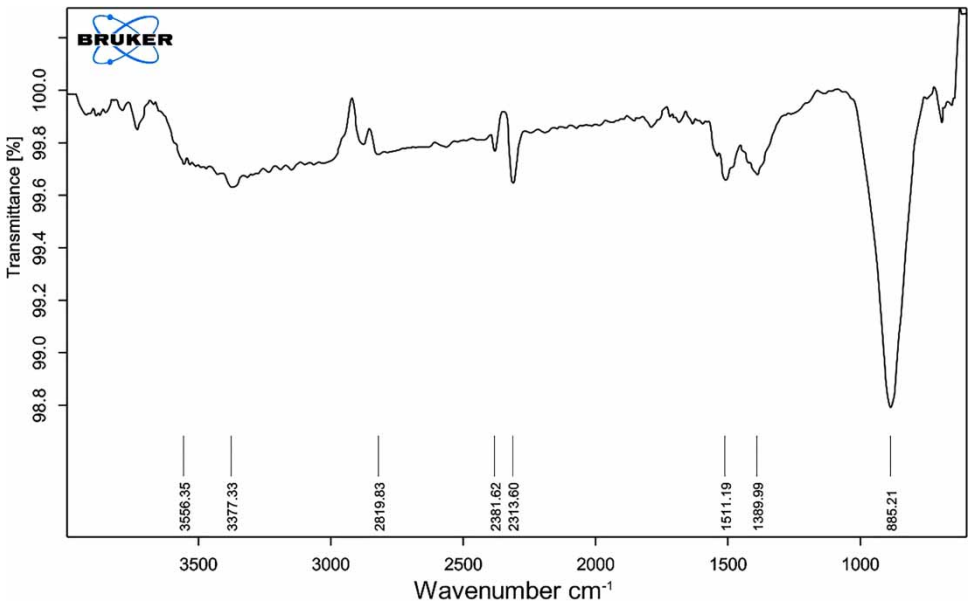

Figure 4 | FTIR of N-doped ZnO.

Figure 4 (Goswami & Sharma 2010; Sahai & Goswami 2014).

In UV-DRS (ultraviolet-diffuse reflectance spectroscopy) (Figure 5), the band gap energy (in eV) of nanoparticles was estimated by employing the Kubelka–Munk (K-M) function (Sahai *et al.* 2014). The band gap of a powder sample can be calculated by plotting $[K/S\ (h\nu)]^2$ against energy (eV). S and K are respectively called as 'K-M scattering' and 'absorption' coefficients (Kubelka & Munk 1931; Pankove 1971). $h\nu$ is the photon energy. Although S and K appear to represent the respective portions of scattered and absorbed lights, per unit vertical length, they have no direct physical meaning on their own. Band gap energy of undoped and N-doped ZnO is found to be 3.30 and 3.13 eV, respectively. Here, N-doped ZnO absorbs longer wavelength (visible light) as compared to undoped ZnO, as its band gap is less. The contribution of nitrogen to the top of the VB of ZnO plays a major role in extending the absorption of N-doped ZnO to the visible region.

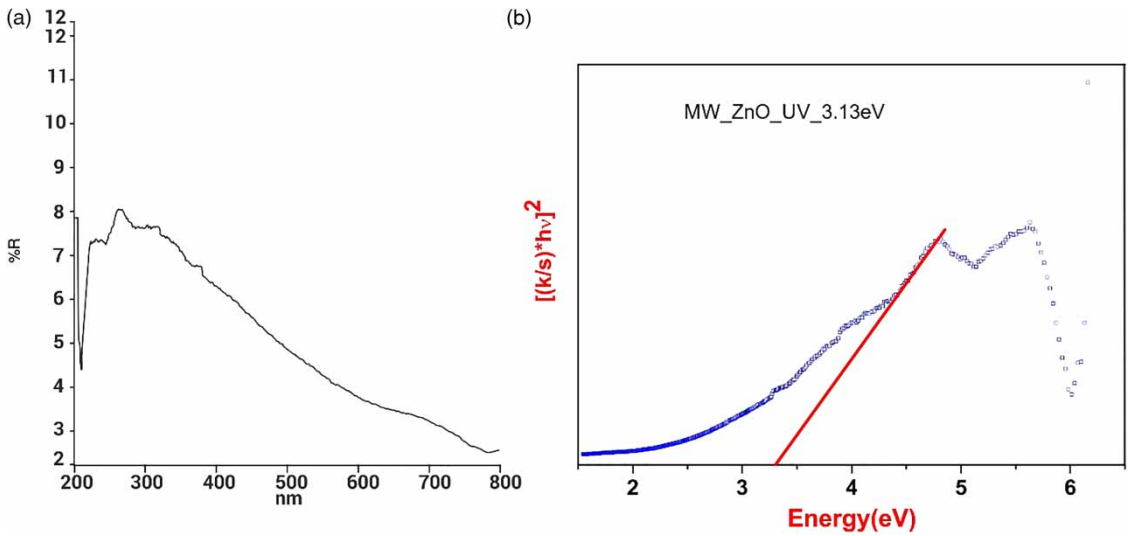

Figure 5 | (a) UV–DRS of N-doped ZnO. (b) Plotting of $[(K/S)\ h\nu]^2$ versus energy (eV) for NZO nanocrystalline thin films by K-M method.

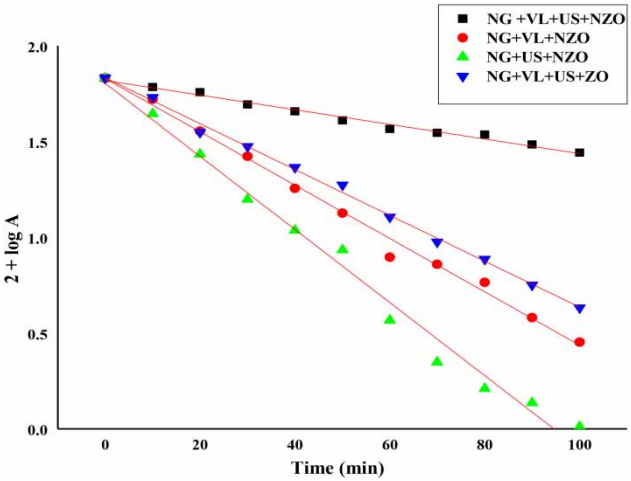

Figure 6 | Typical run.

Typical run

A typical run for the degradation of NG for N-doped ZnO (NZO) and undoped ZnO (ZO) under optimum conditions is reported in Figure 6. It was observed that with increasing time intervals, the absorbance of the solution decreases. This indicates that the concentration of nigrosine dye decreases with increasing exposure duration. A plot of $2 + \log A$ versus time was linear and follows pseudo-first order kinetics. The rate constant was measured using the following expression:

$$k = 2.303 \times \text{Slope} \quad (2)$$

After 100 minutes, the k values were found to be 1.42×10^{-4} (s^{-1}), 5.53×10^{-4} (s^{-1}) and 7.33×10^{-4} (s^{-1}) using NZO for sonocatalysis, photocatalysis and sonophotocatalysis respectively and 4.60×10^{-4} (s^{-1}) using ZO for the sonophotocatalysis process.

Effect of pH variation

The pH was varied between a range of 6 to 9.5 for the sonocatalytic, photocatalytic and sonophotocatalytic degradation of nigrosine dye. It was observed that pH 7.5 was found to be optimum for all the three conditions as shown in Figure 7(a). Both in an acidic and basic medium, the rate of degradation

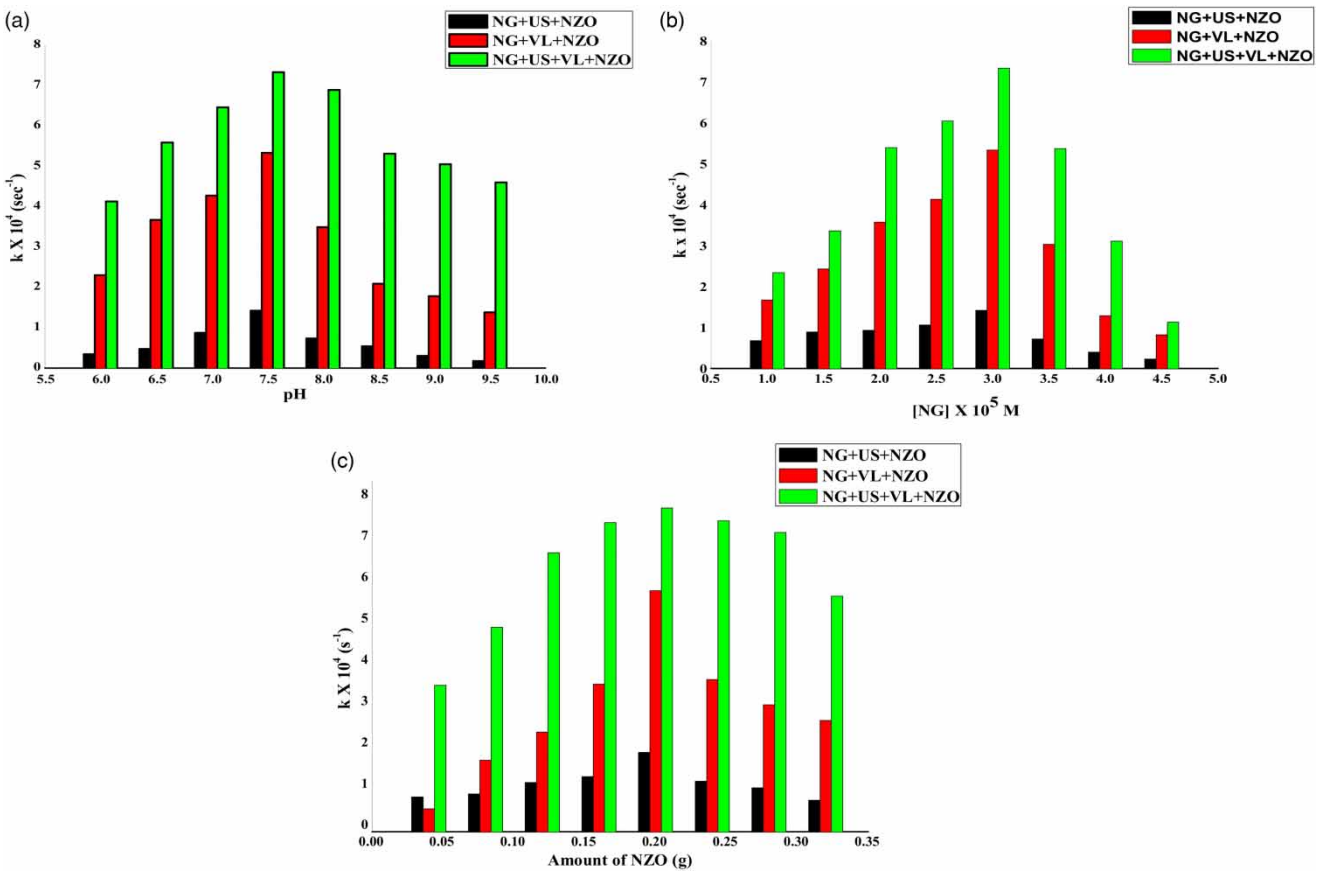

Figure 7 | (a) Effect of pH variation, (b) effect of dye concentration, (c) effect of amount of catalyst.

was substantially decreased. Because at higher pH, the accumulation of hydroxyl radicals and at lower pH, the scavenging of H^+ ions further decrease the activity of the catalyst, hence the rate of removal of dye was also retarded (Spinks & Woods 1990). However, the degradation rate in sonophotocatalysis was higher than that in sonocatalysis and photocatalysis, respectively. This is primarily due to enhanced generation of free radicals via the combined effect of both processes.

Effect of concentration of dye

Keeping all other parameters constant, for nitrogen-doped zinc oxide, the effect of variation of concentration of nigrosine dye on the rate of degradation has been observed in the range from 1.0×10^{-5} M to 4.5×10^{-5} M (Figure 7(b)). It has been observed that the degradation rate increases with increasing concentration of dye up to 3.0×10^{-5} M for all the three cases; that is, sonocatalysis, photocatalysis and sonophotocatalysis. Further increase in concentration beyond this limit results in a decrease in degradation rate. The efficiency of degradation of dye for sonophotocatalysis was found to be highest due to the synergistic effect of both photocatalysis and sonocatalysis. This may be explained on the basis that initially, on increasing the concentration of dye, the reaction rate increases as more molecules of dyes are available for degradation. But further increase in concentration beyond 3.0×10^{-5} M causes retardation of reaction due to increase in the number of collisions between dye molecules and simultaneous decrease in collisions between the dye and $^{\bullet}OH$ radicals. As a consequence, the rate of reaction is retarded. This may be a consequence of the dye starting to act as an internal filter after a particular concentration, not permitting enough light intensity to reach the photocatalyst surface, which is at the bottom of the reaction vessel.

Effect of amount of catalyst

One of the primary parameters that influence the rate of photocatalysis, sonocatalysis and sonophotocatalysis processes is the amount of catalyst. The quantity was varied from 0.04 g to 0.32 g of N-doped ZnO and it was observed that increasing the initial catalyst amount led to an increase in the extent of degradation. The rate almost stabilizes and even slows down gradually after reaching the optimum value of 0.20 g. (Figure 7(c)). This can be attributed to the fact that after the optimum value, the catalyst particles aggregate leading to a reduction in the number of available active surface sites. Beyond a particular loading in a particular reactor, the particles cannot be suspended fully and effectively, which also leads to suboptimal penetration of irradiation and reduced adsorption of the substrate on the surface. Here also the rate of sonophotocatalysis was found to be highest among sonocatalysis and photocatalysis.

Water quality parameters

A number of quality parameters of nigrosine dye sample solution were measured before and after the sonophotocatalytic treatment, as shown in Table 1. Since the best results for the rate of degradation of dye were obtained in sonophotocatalysis, the quality parameters were taken only for sonophotocatalysis.

The COD of the dye solution was determined, both before and after illumination, using the redox method and calculated as per Equation (1). After 100 min of illumination, the efficiency of sonophotocatalytic degradation was found to be 84%.

DO analysis is used to measure the dissolved gaseous oxygen (O_2) in water. The dye was mineralized to a great extent, which was indicated by the increase in the amount of DO from 0.1 ppm to 4.8 ppm, before degradation and after sonophotocatalytic treatment respectively.

Conductivity is directly proportional to the number of ions and hence it can be used as a measure of the ion concentration level of a solution. After the sonophotocatalytic treatment, the conductivity increased, indicating the mineralization of the dye into smaller molecules/ions like CO_2, NO_3^-, SO_4^{2-} etc. For instance, the conductivity of the nigrosine reaction mixture, before and after the sonophotocatalytic treatment, was 21.3 μS and 201 μS, respectively. Also, the salinity and total dissolved solids (TDS) of the dye solution were found to increase to 0.20 ppt (parts per thousand) and 109 ppm (parts per million) from 0.02 ppt to 11.3 ppm respectively.

Prior to treatment, the pH of the reaction mixture was 8.5. However, it becomes neutral (7.12) after sonophotocatalytic

Table 1 | Various water quality parameters

Various parameters	Before sonophotocatalytic treatment NZO	After sonophotocatalytic treatment NZO
COD (mg/L)	523	82.3
DO (ppm)	0.1	4.8
Conductance (μS)	21.3	201
Salinity (ppt)	0.02	0.20
TDS (ppm)	11.3	109
pH	8.5	7.12

degradation of the dye, which clearly demonstrates the mineralization of the dye particles to a significant extent.

Mechanism

On the basis of the experimental observation, the following tentative mechanism has been proposed for sonophotocatalytic degradation of NG. The NG dye molecule absorbs radiation of suitable wavelengths and it is excited to its first singlet excited state followed by intersystem crossing (ISC) to the triplet state.

$$^1NG_0 + hv \longrightarrow {}^1NG_1 \quad \text{(Singlet excited state)} \tag{3}$$

$$^1NG_1 \xrightarrow{ISC} {}^3NG_1 \quad \text{(Triplet excited state)} \tag{4}$$

The semiconductor (SC) will be excited on exposure to visible light and/or ultrasound to give SC*. This excited state will provide an electron (e^-) in the conduction band and a hole in the VB. This hole may abstract an electron from hydroxyl ions to generate hydroxyl radicals. These hydroxyl radicals will then oxidize the dye molecules to harmless products. The same reaction was carried out in the presence of isopropanol, a hydroxyl radical scavenger, to ascertain the role of $^{\bullet}OH$ radicals as an active oxidizing species. The rate of degradation reduced drastically, thus confirming the active oxidizing species as $^{\bullet}OH$ radicals.

$$SC + hv \longrightarrow e^-(CB) + h^+(VB) \tag{5}$$

$$h^+ + OH \longrightarrow {}^{\bullet}OH \tag{6}$$

$$^{\bullet}OH + {}^3NG_1 \longrightarrow \text{Smaller products like } CO_2, NO_3^-, NO_2^-, SO_3^{2-}, SO_4^{2-} \text{ etc} \tag{7}$$

The generation of more $^{\bullet}OH$ radicals in the presence of ultrasound by sonolysis of water will add to the degradation rate of nigrosine dye.

$$H_2O \xrightarrow{))))} H^{\bullet} + {}^{\bullet}OH \tag{8}$$

CONCLUSIONS

The conclusions of this study are given below.

- This study reveals that ultrasonication has been able to accelerate the degradation process under visible light.
- The degradation of the commercial textile dye named nigrosine (NG) was investigated by sonophotocatalytic, photocatalytic and sonocatalytic processes under different operating conditions like effect of pH, initial dye concentration and catalyst loading in an aqueous solution. The efficiency of the degradation process is affected by the amount of photocatalyst, concentration of nigrosine dye and the initial pH of the solution.
- Under optimum conditions, 3.0×10^{-5} M of nigrosine dye can be effectively degraded by 4.0 g L^{-1} of N-doped ZnO at pH 7.5.
- COD studies show that 84% of dye is removed from the solution during irradiation time. This study indicates the great potential of N-doped ZnO to mineralize nigrosine dye under both UV and US conditions.
- An additional advantage of this methodology is that it can harness the technique using solar energy for the degradation of organic pollutants in water. Studies are in progress to apply this synergistic technique using visible light. As one of the green benign approaches, sonophotocatalysis appears to be the most promising process for the decontamination of commercially viable pollutants from the effluents of various industries under ambient conditions.

ACKNOWLEDGEMENTS

The authors extend their heartfelt gratitude to DST-FIST schemes (Department of Science and Technology-Fund for Improvement of S&T infrastructure in universities and higher educational institutions) of the Department of Physics, M. L. Sukhadia University, Udaipur, for providing XRD characterization facilities. We are also thankful to UGC-DAE (University Grant Commission-Department of Atomic Energy) Consortium for Scientific Research, Indore for providing TEM facility and SAIF (Sophisticated Analytical Instrumentation Facility) Chandigarh for providing FESEM, EDX, UV-DRS facilities. We also sincerely thank the Head, Department of Chemistry, M. L. Sukhadia University, Udaipur, for providing access to laboratory facilities.

REFERENCES

Al-Ekabi, H. & Serpone, N. 1988 Kinetic-studies in heterogeneous photocatalysis. 1. Photocatalytic degradation of chlorinated phenols in aerated aqueous solutions over TiO_2 supported on a glass matrix. *Journal of Physical Chemistry* **92**, 5726–5731.

Anju, S. G., Yesodharan, S. & Yesodharan, E. P. 2012 Zinc oxide mediated sonophotocatalytic degradation of phenol in water. *Chemical Engineering Journal* **189–190**, 84–93.

Azbar, N., Yonar, T. & Kestioglu, K. 2004 Comparison of various advanced oxidation processes and chemical treatment methods for COD and color removal from a polyester and acetate fiber dyeing effluent. *Chemosphere* **55**, 35–43.

Chakma, S. & Moholkar, V. S. 2013 Numerical simulation and investigation of system parameters of sonochemical process. *Chinese Journal of Engineering* **2013**, 362682.

Chen, Y. C. & Smirniotis, P. 2002 Enhancement of photocatalytic degradation of phenol and chlorophenols by ultrasound. *Industrial & Engineering Chemical Research* **41** (24), 5958–5969.

Comninellis, C., Kapalka, A., Malato, S., Parsons, S. A., Poulios, l. & Mantzavinos, D. 2008 Advanced oxidation processes for water treatment: advances and trends for R&D. *Journal of Chemical Technology and Biotechnology* **83**, 769–776.

Gogate, P. R. 2008 Treatment of wastewater streams containing phenolic compounds using hybrid techniques based on cavitation: a review of the current status and the way forward. *Ultrasonics Sonochemistry* **15**, 1–15.

Goswami, N. & Sharma, D. K. 2010 Structural and optical properties of unannealed and annealed ZnO nanoparticles prepared by a chemical precipitation technique. *Physica E: Low-Dimensional Systems and Nanostructures* **42**, 1675–1682.

Hoffman, M. R., Martin, S. T., Choi, W. & Bahnemann, W. 1995 Environmental applications of semiconductor photocatalysis. *Chemical Reviews* **95**, 69–96.

Joseph, C. G., Puma, G. L., Bono, A. & Krishniah, D. 2009 Sonophotocatalysis in advanced oxidation process: a short review. *Ultrasonics Sonochemistry* **16**, 583–589.

Kandavelu, V., Kastien, H. & Thampi, K. R. 2004 Photocatalytic degradation of isothiazolin-3-ones in water and emulsion paints containing nanocrystalline TiO_2 and ZnO catalysts. *Applied Catalysis B* **48**, 101–111.

Khataee, A., Karimi, A., Arefi-Oskoui, S., Darvishi, C. S. R., Hanifehpour, Y., Soltani, B. & Joo, S. W. 2015 Sonochemical synthesis of Pr-doped ZnO nanoparticles for sonocatalytic degradation of acid red 17. *Ultrasonics Sonochemistry* **22**, 371–381.

Kooti, M. & Sedeh, A. N. 2013 Microwave-assisted combustion synthesis of ZnO nanoparticles. *Journal of Chemistry* **2013**, 4.

Kubelka, P. & Munk, F. 1931 An article on optics of paint layers. *Zeitschrift für Technische Physik* **12**, 593–601.

Lu, J., Zhang, Q., Wang, J., Saito, F. & Uchida, M. 2006 Synthesis of N-doped ZnO by grinding and subsequent heating ZnO-urea mixture. *Powder Technology* **162**, 33–37.

Mollavali, M., Falamaki, C. & Rohani, S. 2018 Efficient light harvesting by NiS/CdS/ZnS NPs incorporated in C, N-co-doped-TiO_2 nanotube arrays as visible-light sensitive multilayer photoanode for solar applications. *International Journal of Hydrogen Energy* **43**, 9259–9278.

Pankove, J. I. 1971 *Optical Processes in Semiconductors*. Dover Publications Inc., New York, NY, USA.

Periyat, P. & Ullattil, S. G. 2015 Sol–gel derived nanocrystalline ZnO photoanode film for dye sensitized solar cells. *Materials Science in Semiconductor Processing* **31**, 139–146.

Pimentel, A., Nunes, D. & Duarte, P. 2014 Synthesis of long ZnO nanorods under microwave irradiation or conventional heating. *Journal of Physical Chemistry C* **118** (26), 14629–14639.

Robinson, T., McMullan, G., Marchant, R. & Nigam, P. 2001 Remediation of dyes in textile effluent: a critical review on current treatment technologies with a proposed alternative. *Bioresource Technology* **77** (3), 247–255.

Sahai, A. & Goswami, N. 2014 Structural and vibrational properties of ZnO nanoparticles synthesized by the chemical precipitation method. *Physica E: Low-Dimensional Systems and Nanostructures* **58**, 130–137.

Sahai, A., Kumar, Y., Agarwal, V., Olive-Mendez, S. & Goswami, N. 2014 Doping concentration driven morphological evolution of Fe doped ZnO nanostructures. *Journal of Applied Physics* **116** (16), 164315.

Saratale, R. G., Saratale, G. D., Chang, J. S. & Govindwar, S. P. 2011 Bacterial decolorization and degradation of azo dyes: a review. *Journal of the Taiwan Institute of Chemical Engineers* **42**, 138–157.

Seguel, G. V., Rivas, B. L. & Novas, C. 2005 Polymeric ligand-metal acetate interactions: spectroscopic study and semi-empirical calculations. *Journal of Chilean Chemical Society* **50**, 401–406.

Seo, H. K. & Shin, H. S. 2015 Study on photocatalytic activity of ZnO nanodisks for the degradation of rhodamine B dye. *Materials Letters* **159**, 265–268.

Shah, Y. T., Pandit, A. B. & Moholkar, V. S. 1990 *Cavitation Reaction Engineering*. Kluwer Academic: Plenum Publishers, New York, NY, USA.

Singh, R., Kumar, M., Khajuria, H., Ladol, J. & Sheikh, H. N. 2018 Solvothermal synthesis of ZnO-nitrogen doped graphene composite and its application as catalyst for photodegradation of organic dye methylene blue. *Acta Chimica Slovenica* **65**, 319–327.

Spinks, J. W. T. & Woods, R. J. 1990 *An Introduction to Radiation Chemistry*, 3rd edn. John Wiley & Sons, New York.

Su, Y. C., Chiou, C. C., Marinova, V., Lin, S. H., Bozhinov, N., Blagoev, B., Babeva, T., Hsu, K. Y. & Dimitrov, D. Z. 2018 Atomic layer deposition prepared Al-doped ZnO for liquid crystal displays applications. *Optical and Quantum Electronics* **50**, 205.

Torres-Palma, R. A., Nieto, J. I., Combet, E. & Petrier, C. 2010 An innovative ultrasound, Fe^{2+} and TiO_2 photoassisted process for bisphenol a mineralization. *Water Research* **44**, 2245–2252.

Willey, J. M., Sherwood, L., Woolverton, C. J. & Prescott, L. M. 2009 *Prescott's Principles of Microbiology*. McGraw-Hill Higher Education, Boston, MA, USA.

Xu, S., Zhang, X., Ng, J. & Sun, D. D. 2009 Preparation and application of TiO_2/Al_2O_3. *Water Science & Technology Water Supply* **9**, 39–44.

Zhu, L., Meng, Z. D., Park, C. Y., Ghosh, T. & Oh, W. C. 2013 Characterization and relative sonocatalytic efficiencies of a new MWCNT and CdS modified TiO_2 catalysts and their application in the sonocatalytic degradation of rhodamine B. *Ultrasonics Sonochemistry* **20**, 478–484.

First received 7 May 2019; accepted in revised form 22 November 2019. Available online 2 December 2019